

# Exact steady state of perturbed open quantum systems

Omar Nagib\* and T. G. Walker

*Department of Physics, University of Wisconsin-Madison, 1150 University Avenue, Madison, WI, 53706, USA*

(Dated: January 13, 2025)

We present a general non-perturbative method to determine the exact perturbed steady state of open quantum systems, in terms of the eigenmodes of the unperturbed system. The perturbation may be time-independent or periodic, and of arbitrarily large amplitude. Using a generalized inverse and two diagonalizations, we construct an operator that generates the entire dependence of the steady state on the perturbation parameter. The approach also enables exact analytic operations—such as differentiation, integration, and ensemble averaging—with respect to the parameter, even when the steady state is computed numerically. We apply the method to three non-trivial open quantum systems, showing that it achieves exact results, with a computational speedup for calculations requiring large sampling, such as ensemble averaging, compared to sampling-based approaches.

## I. INTRODUCTION

Many quantum processes, such as photochemistry, energy transport, quantum optics, electronic and spin resonance, quantum computing and sensing, are described by a quantum master equation [1]. Finding the steady state of such open quantum systems is a problem of great theoretical and practical interest. For sufficiently large and complicated systems, only numerical solutions are possible. Consequently, many numerical approaches have been developed, including eigenvalue methods and LU decomposition [2], variational principles [3], neural networks [4], quantum trajectories [5, 6], matrix product density operators [7], and iterative methods [8], to name a few (see [1, 2, 9] and the references within for a review). Numerical tools for efficient simulation of open quantum systems have also been created, such as QuTiP, HOQST, SPINACH, Julia (Quantumoptics.j), and RydIQule [10–14].

After finding the steady state, it is often desirable to study the dependence of the steady state on some parameter  $v$ , which appears in the Hamiltonian or dissipator. This includes direct dependence on, rate of change with, or an ensemble average over  $v$ , e.g., Doppler broadening in atomic systems [15] or static disorder in condensed matter systems [6]. In the absence of analytic solutions, it is often required to sample over  $v$  and find the steady state for every distinct value. This process is computationally expensive in time and memory. Furthermore, analytic operations, e.g., differentiation and integration with respect to  $v$ , must be approximated by the corresponding discretized ones, e.g., finite differences and Riemann sums. Reducing the error in these operations necessitates a larger sample size in  $v$ , so there is a trade-off between the error and computational memory and speed. This presents a computational bottleneck for large open quantum systems.

In the formalism of quantum master equations, the system's Liouville superoperator  $\mathcal{L}$  (also known as the Lind-

bladian) contains all the information about the Hamiltonian and dissipation [1]. Consider the common case where the Lindbladian can be decomposed into two parts  $\mathcal{L} = \mathcal{L}_0 + v\mathcal{L}_1$ , for some parameter  $v$ . This decomposition arises naturally in perturbation theory [16–19] and linear response theory, where  $\mathcal{L}_0$  is the original system, and  $v\mathcal{L}_1$  is some perturbation. Perturbation theory on open quantum systems has been applied previously in various settings with success, e.g., many-body systems [20, 21], quantum transport [22], and laser cooling of trapped ions [23]. More generally, systematic perturbative expansions have been developed for open quantum systems with small dissipation [17, 24, 25]. When combined with adiabatic elimination, perturbation theory can create a simplified effective Liouville superoperator, which only involves the ground states' degrees of freedom [26–28]. Perturbation theory on open quantum systems has also been used to derive a generalized Kubo formula, which captures the response theory of observables under a perturbation [29–31].

A general perturbation theory for open quantum systems was introduced by Li et al. [32]. Given the steady state  $\rho_0$  of  $\mathcal{L}_0$ , the theory calculates the perturbed steady state  $\rho_v$  of  $\mathcal{L}_0 + v\mathcal{L}_1$  up to any desired power in  $v$ . In an extension of their work, the authors introduced a partial resummation scheme of the infinite perturbative series for the steady state, where each term in the sum contains corrections up to the infinite order [33]. While this work represents a significant improvement over finite-order perturbation theory, it is still perturbative and approximate, because the formal infinite series solution has to be truncated for any practical calculation. In addition to being inherently approximate, perturbation theory can fail even for small perturbations [20] and determining the domain of convergence is a non-trivial problem [32, 34].

Going beyond perturbation theory, we use the diagonalization of  $\mathcal{L}_0$  to generate an exact non-perturbative solution for the steady state  $\rho_v$ , for an arbitrary time-independent or periodic perturbation. We show that by diagonalizing the product of a generalized inverse of  $\mathcal{L}_0$  and  $\mathcal{L}_1$ , the exact  $v$ -dependence of  $\rho_v$  can be efficiently obtained. This method is applicable to a wide variety of

\* onagib@wisc.edu

open quantum systems. We give three examples in this paper.

In Sec. II, a summary of the the problem is given, as well as a sketch of the main result. In Sec. III, the main result is derived, which is inspired by Green's function: given the  $v = 0$  solution  $\rho_0$ , we derive the ‘‘propagator’’ that acts on ‘‘zero-case’’ state to generate the general  $v$ -dependent solution  $\rho_v$ . The exact non-perturbative solution for all  $v$  can be found just by two matrix diagonalizations, of  $\mathcal{L}_0$  and  $\mathcal{L}_0^- \mathcal{L}_1$ , where  $\mathcal{L}_0^-$  is a trace-preserving generalized inverse of  $\mathcal{L}_0$ . Our derivation is general and does not assume a perturbative series solution. Furthermore, this approach allows for exact analytic operations, such as differentiation and ensemble averaging on  $\rho_v$  with respect to  $v$ , without the need for discretization or sampling. The reduction of the number of diagonalizations to two can lead to savings in computational time and memory, while still being exact. This approach works even if the system can only be solved numerically. To showcase its validity and utility, we apply the present method to three non-trivial open quantum systems. In Sec. IV, we compute the dependence of cavity optomechanical cooling on the pump laser frequency, just by doing two diagonalizations. In Sec. V, we compute the non-linear response of an atomic magnetometer. In Sec. VI, we compute the velocity dependence and calculate Doppler broadening of a modulated multi-level Rydberg sensor at room temperature, without any sampling. We find agreement between the present method and the exact and numerical solutions for all these systems. For ensemble averaging calculations, such as Doppler broadening, the present method achieves a speedup of one to several orders of magnitude, compared to numerical sampling. This approach works for the steady-state solutions of systems with no or periodic time-dependence, and hence it is expected to be of wide applicability. Sec. VII concludes with a discussion.

## II. PROBLEM SETUP AND SUMMARY

We consider a quantum system whose time evolution is governed by a quantum master equation. In the superoperator form, it is given by [1]:

$$\dot{\rho} = \mathcal{L}\rho \quad (1)$$

where  $\rho$  is the ‘‘vectorized’’ version of the density matrix  $\rho$ , and  $\mathcal{L}$  is the Liouville superoperator. A vectorization  $\text{vec}(\rho)$  maps the density matrix  $\rho = \sum_{ij} \rho_{ij} |i\rangle \langle j|$  into the column vector  $\rho = \text{vec}(\rho) = \sum_{ij} \rho_{ij} |i\rangle \otimes |j\rangle$ .  $\mathcal{L}$  is constructed from the Hamiltonian  $H$  and the Lindblad operators  $L_k$  that couple the system to the environment, causing dissipation and decoherence. See Appendix A for an overview of the Liouville superoperator formalism as used in this work. The particular form of  $\mathcal{L}$  depends on the nature of the coupling between the system and the environment. For Markovian dynamics, it is given by the

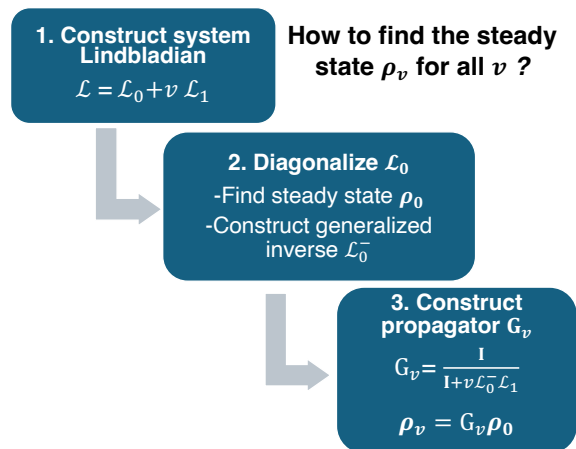


FIG. 1. The procedure to find the steady state  $\rho_v$  of an open quantum system, as a function of any system parameter  $v$ . Once the propagator is constructed,  $\rho_v$  is found for all  $v$  as well as any analytic operation (e.g., integration and differentiation) on  $\rho_v$  can be done exactly.

Lindblad form:

$$\mathcal{L} = -i(H \otimes \mathbb{1} - \mathbb{1} \otimes H^T) + \sum_k (L_k \otimes L_k^* - \frac{1}{2} [L_k^\dagger L_k \otimes \mathbb{1} + \mathbb{1} \otimes L_k^T L_k^*]) \quad (2)$$

At steady state, Eq. (1) becomes  $\mathcal{L}\rho = 0$ , and finding the steady state reduces to finding the nullspace vector of  $\mathcal{L}$ . Now consider a quantity  $v$  in the Hamiltonian or the Lindblad operators, such that  $\mathcal{L}$  is divided into two parts:

$$\mathcal{L}\rho_v = (\mathcal{L}_0 + v\mathcal{L}_1)\rho_v = 0 \quad (3)$$

where both  $\mathcal{L}_0$  and  $\mathcal{L}_1$  do not depend on  $v$ . Suppose that a unique steady-state solution exists for the zero-case problem, i.e.,  $\mathcal{L}_0\rho_0 = 0$ , which is available either analytically or numerically. The question is how to find the  $v$ -dependent solution  $\rho_v$  in terms of  $\rho_0$ . More generally, the goal is to find a procedure to do analytic operations exactly with respect to  $v$  even if  $\rho_v$  is only available numerically, e.g., find the ensemble average of  $\rho_v$  over a probability distribution, i.e.,  $\bar{\rho} = \int P(v)\rho_v dv$ . Both the steady state and time evolution of  $\rho_v$  have been previously handled using approximate methods such as perturbation theory [17, 18, 32, 33].

Fig. 1 pictorially summarizes the main result. We efficiently construct a propagator  $G_v$  that acts on the zero-case solution  $\rho_0$  to generate the  $v$ -dependent general solution for all  $v$ , i.e.,  $G_v\rho_0 = \rho_v$ . Once  $G_v$  is constructed, not only  $\rho_v$  is found exactly, but analytic operations, such as differentiation and integration, can be done exactly on  $\rho_v$ , without any sampling. In the next section, we derive  $G_v$  and show how to construct it.

### III. PROPAGATOR APPROACH TO THE NULLSPACE OF THE MASTER EQUATION

In this section, we show that the propagator  $G_v$  that generates the  $v$ -dependent nullspace is

$$G_v = (\mathbb{1} + v\mathcal{L}_0^- \mathcal{L}_1)^{-1} \equiv \frac{\mathbb{1}}{\mathbb{1} + v\mathcal{L}_0^- \mathcal{L}_1} \quad (4)$$

where  $\mathcal{L}_0^-$  is a generalized inverse of  $\mathcal{L}_0$ , to be defined shortly. Let  $\mathbf{R}_g$  and  $\mathbf{L}_g$  be the right and left column eigenvectors of  $\mathcal{L}_0$ , and  $g$  be the corresponding complex eigenvalues. The right and left eigenvectors of  $\mathcal{L}_0$  obey the following eigenvalue, orthonormality, and completeness relations

$$\mathcal{L}_0 \mathbf{R}_g = g \mathbf{R}_g \quad (5a)$$

$$\mathbf{L}_g^T \mathcal{L}_0 = g \mathbf{L}_g^T \quad (5b)$$

$$\mathbf{L}_i^T \mathbf{R}_j = \delta_{ij} \quad (5c)$$

$$\sum_g \mathbf{R}_g \mathbf{L}_g^T = \mathbb{1} \quad (5d)$$

In other words, we consider quantum systems that admit an eigendecomposition  $\mathcal{L}_0 = \sum_g g \mathbf{R}_g \mathbf{L}_g^T$ , where the matrix multiplication  $\mathbf{R}_g \mathbf{L}_g^T$  is mathematically equivalent to  $\mathbf{R}_g \otimes \mathbf{L}_g^T$ . We shall assume that a unique steady state exists, which is given by the right nullspace vector of  $\mathcal{L}_0$ , i.e.,  $\mathbf{R}_0 = \boldsymbol{\rho}_0$ . The left nullspace vector,  $\mathbf{L}_0$ , is the same for all  $\mathcal{L}_0$  in quantum systems to ensure probability conservation with time. More precisely, the left nullspace vector is the vectorization of the identity, i.e.,  $\mathbf{L}_0 = \text{vec}(\mathbb{1})$  for all quantum systems (see Appendix A) [35].  $\mathcal{L}_0^-$  is then defined as the inverse of  $\mathcal{L}_0$  excluding the zero-eigenvector (nullspace):

$$\mathcal{L}_0^- = \sum_{g \neq 0} \frac{1}{g} \mathbf{R}_g \mathbf{L}_g^T \quad (6)$$

where  $\mathcal{L}_0$  and  $\mathcal{L}_0^-$  obey the generalized inverse relations

$$\mathcal{L}_0 \mathcal{L}_0^- = \mathcal{L}_0^- \mathcal{L}_0 = \mathbb{1} - \mathbf{R}_0 \mathbf{L}_0^T \quad (7)$$

It is important to point out that since  $\mathcal{L}_0 \mathcal{L}_0^-$  and  $\mathcal{L}_0^- \mathcal{L}_0$  are not Hermitian matrices,  $\mathcal{L}_0^-$  is not the Moore-Penrose inverse of  $\mathcal{L}_0$ . In the mathematics literature,  $\mathcal{L}_0^-$  is called the ‘‘semi-inverse’’, ‘‘reciprocal inverse’’, or ‘‘reflexive generalized inverse’’, i.e. it obeys  $\mathcal{L}_0 \mathcal{L}_0^- \mathcal{L}_0 = \mathcal{L}_0$  and  $\mathcal{L}_0^- \mathcal{L}_0 \mathcal{L}_0^- = \mathcal{L}_0^-$  [36]. In Appendix B1, we show how to efficiently construct  $\mathcal{L}_0^-$ .

Next, we prove that this propagator generates  $\boldsymbol{\rho}_v$ . Acting on Eq. (3) with  $\mathcal{L}_0^-$  and using Eq. (7) gives

$$\mathcal{L}_0^- (\mathcal{L}_0 + v\mathcal{L}_1) \boldsymbol{\rho}_v = (\mathbb{1} - \mathbf{R}_0 \mathbf{L}_0^T + v\mathcal{L}_0^- \mathcal{L}_1) \boldsymbol{\rho}_v \quad (8)$$

Using the identity  $\mathbf{L}_0^T \boldsymbol{\rho}_v = \text{vec}(\mathbb{1})^T \cdot \boldsymbol{\rho}_v = \text{Tr}(\boldsymbol{\rho}_v) = 1$ , which is a statement of probability conservation (see Appendix A for proof) [35], setting  $\mathbf{R}_0 = \boldsymbol{\rho}_0$ , and rearranging, we get:

$$(\mathbb{1} + v\mathcal{L}_0^- \mathcal{L}_1) \boldsymbol{\rho}_v = \boldsymbol{\rho}_0 \quad (9)$$

Inverting this equation readily gives:

$$\boldsymbol{\rho}_v = \frac{\mathbb{1}}{\mathbb{1} + v\mathcal{L}_0^- \mathcal{L}_1} \boldsymbol{\rho}_0 \quad (10)$$

which shows that Eq. (4) indeed gives the correct propagator. This equation can be generalized for the case of more than one variable  $\{v_i\}$ , as described in Appendix B2.

To be able to deal analytically with Eq. (4), we diagonalize  $\mathcal{L}_0^- \mathcal{L}_1$  to find its right and left eigenvectors,  $\mathbf{r}_\lambda$  and  $\mathbf{l}_\lambda$ , and their corresponding eigenvalues  $\lambda$ . Then the eigendecomposition of the propagator in that basis gives:

$$G_v = \sum_{\lambda=\lambda_1}^{\lambda_N} \frac{1}{1 + \lambda v} \mathbf{r}_\lambda \mathbf{l}_\lambda^T \quad (11a)$$

$$\boldsymbol{\rho}_v = G_v \boldsymbol{\rho}_0 \quad (11b)$$

$G_v$  can be constructed efficiently, as shown in Appendix B3. Due to the choice of the generalized inverse, which is trace-persevering,  $\boldsymbol{\rho}_v$  is automatically normalized if  $\boldsymbol{\rho}_0$  is normalized. We have obtained an exact non-perturbative solution for an arbitrary perturbation  $v\mathcal{L}_1$ , generated from the unperturbed steady state. The problem of finding the arbitrary steady state for all  $v$  has thus been reduced to two diagonalizations: diagonalizing  $\mathcal{L}_0$  (the zero-case problem) and  $\mathcal{L}_0^- \mathcal{L}_1$  (the auxiliary problem). These diagonalizations, in turn, can be done either numerically or analytically. Once these two problems are solved,  $\boldsymbol{\rho}_v$  follows immediately from Eqs. (11a) and (11b), without the need to redo the diagonalization for every distinct  $v$ .

It is important to emphasize the generality of this derivation: no assumptions were made about the magnitude of  $v$  or whether  $\boldsymbol{\rho}_v$  admits a perturbative expansion in  $v$ . In Appendix C, we elaborate on the relation between this method and perturbation theory on open quantum systems, showing that this method gives the exact result even when no corresponding perturbation theory is possible. For cases where a perturbative expansion exists, the solution is equivalent to perturbation theory with corrections up to the infinite order. Therefore, this solution goes well beyond perturbation theory [32, 33].

In addition to being exact, the present method can offer computational speedup in many cases. In the approach where  $\boldsymbol{\rho}_v$  is found by repeatedly computing the nullspace vector for every  $v$  [Eq. (3)], the computational time is expected to grow linearly with the number of samples in  $v$ . Under the present method, on the other hand, there is a constant overhead associated with the two diagonalizations, of  $\mathcal{L}_0$  and  $\mathcal{L}_0^- \mathcal{L}_1$ , independent of the number of samples in  $v$ , after which any  $\boldsymbol{\rho}_v$  can be generated efficiently. In other words, the present method can offer computational speedup when the time to diagonalize  $\mathcal{L}_0$  and  $\mathcal{L}_0^- \mathcal{L}_1$  is much less than the time taken to find  $\boldsymbol{\rho}_v$  by repeatedly solving for the nullspace. There-

fore, this approach can lead to speedup in computational time for problems that require many samples of  $v$ .

Since  $v$  appears in a simple form in Eq. (11a), analytic operations with respect to  $v$  on  $\rho_v$  can be done exactly, e.g., differentiation and integration with respect to  $v$ . These operations can be done exactly, even when only a numerical solution is available, without the need to approximate these operations using finite differences and Riemann sums. For example, an ensemble average can be analytically computed by integrating the  $v$ -dependence in  $G_v$ , i.e.,  $\int dv P(v) 1/(1 + \lambda v)$ . We obtain the ensemble average exactly without any approximations, while simultaneously saving significant computational resources by avoiding sampling over  $v$ . For the case where  $P(v)$  is a Gaussian distribution with a standard deviation  $\sigma_v$ , i.e.,  $P(v) = (2\pi\sigma_v^2)^{-1/2} \exp(-v^2/2\sigma_v^2)$ , the  $v$ -dependence is integrated, and we get the ensemble-averaged steady state

$$\begin{aligned} \bar{\rho} &= \sum_{\lambda=0} (\mathbf{r}_\lambda \mathbf{l}_\lambda^T) \rho_0 \\ &+ \sum_{\lambda \neq 0} \frac{\sqrt{\pi/2}}{\sqrt{-\lambda^2 \sigma_v}} e^{-\frac{1}{2\lambda^2 \sigma_v^2}} \left( 1 + \operatorname{erf} \left[ \frac{\sqrt{-\lambda^2}}{\sqrt{2}\lambda^2 \sigma_v} \right] \right) (\mathbf{r}_\lambda \mathbf{l}_\lambda^T) \rho_0 \end{aligned} \quad (12)$$

where erf is the Error function, and the first and the second sums are over the zero and non-zero eigenvalues  $\lambda$ , respectively. In Appendix D, we calculate Doppler broadening for a two-level system, for which an exact solution is analytically available, showing agreement between the present and the analytic solutions. In Appendix E, we explicitly compute the ensemble average for a Lorentzian distribution. This approach can also be applied to compute the exact ensemble average with respect to any other desired distribution.

In the next sections, we apply this approach to three non-trivial open quantum systems, showing that it agrees with the exact results, as well as achieving computational speedup for calculations that require large sampling.

#### IV. EXAMPLE 1: CAVITY OPTOMECHANICAL COOLING

The standard Hamiltonian coupling a laser-driven optical cavity to a mechanical oscillator, in a frame rotating with the laser frequency, is given by [38, 39]

$$H = -\Delta a^\dagger a + \omega_m b^\dagger b - g_0 a^\dagger a (b + b^\dagger) + \eta (a + a^\dagger) \quad (13)$$

where  $a$  ( $b$ ) is the annihilation operator for the cavity (mechanical oscillator), and  $g_0$  is the vacuum coupling strength between the cavity and the oscillator.  $\omega_c$  ( $\omega_m$ ) is the cavity (oscillator) resonance frequency,  $\Delta = \omega_L - \omega_c$  is the detuning between the driving laser and the cavity, and  $\eta$  is the laser pump strength. There is a Lindblad operator associated with the cavity photon losses  $L_c$ , as well as operators  $L_m^\pm$  that couple the oscillator to a ther-

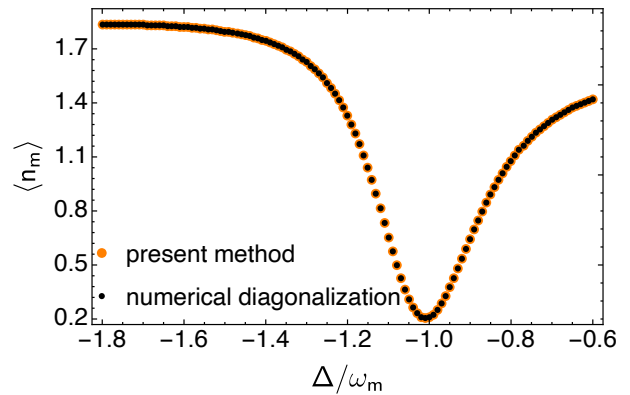


FIG. 2. Phonon number  $\langle n \rangle_m$  at steady state versus detuning  $\Delta$ , using the present method (orange) and numerical diagonalization (black). The system parameters used are (arbitrary units):  $\omega_m = 10$ ,  $g = 1$ ,  $\eta = 2$ ,  $\kappa = 1$ ,  $\Gamma_m = 0.015$ , and  $n_{\text{th}} = 2$ , where the parameters choice was inspired from Ref. [37]. Fock space dimensions of  $N_m = 10$  and  $N_c = 4$  were used for the simulation of the oscillator and the cavity, respectively. Using the present method, the entire plot has been generated using only two diagonalizations.

mal bath:

$$L_c = \sqrt{\kappa} a \quad (14a)$$

$$L_m^+ = \sqrt{\Gamma_m n_{\text{th}}} b^\dagger \quad (14b)$$

$$L_m^- = \sqrt{\Gamma_m (n_{\text{th}} + 1)} b \quad (14c)$$

where  $\kappa$  is the cavity decay rate,  $\Gamma_m$  is the mechanical damping rate, and  $n_{\text{th}}$  is the average thermal phonon number. When  $\Delta = -\omega_m$  and  $\omega_m \gg \kappa$ , the cavity and the oscillator have the same resonance frequencies and can interchange photons and phonons. As the phonons get transferred as photons into the cavity, they are subsequently expelled outside the system. This mechanism leads to cooling of the oscillator. Increasing the pump strength  $\eta$  enhances the effective interaction strength between the two resonators, driving the steady-state phonon number down [38, 39].

Here, we apply the present method to compute the dependence of the steady-state average phonon number  $\langle n_m \rangle$  on the laser detuning  $\Delta$ .  $\mathcal{L}_0$  is constructed from  $H$  and the Lindblad operators [Eqs. (13) and (14)] with  $\Delta = -\omega_m$ , using Eq. (2).  $\mathcal{L}_0$  is numerically diagonalized, where its nullspace gives the steady state at  $\Delta = -\omega_m$ . Next the generalized inverse  $\mathcal{L}_0^-$  is constructed [Eq. (6)]. To find the steady state  $\rho_\delta$  at any other detuning  $\delta$  away from  $\omega_m$ , i.e.,  $\Delta = -\omega_m + \delta$ , we note that the corresponding part in the Hamiltonian,  $-\Delta a^\dagger a$ , can be decomposed as  $\omega_m a^\dagger a - \delta a^\dagger a$ . Thus, we make the identification  $H_1 = -a^\dagger a$  and construct  $\mathcal{L}_1$ . Finally, we numerically diagonalize  $\mathcal{L}_0^- \mathcal{L}_1$  to find the propagator  $G_\delta$  [Eq. (11a)], which generates the  $\delta$ -dependent exact solution

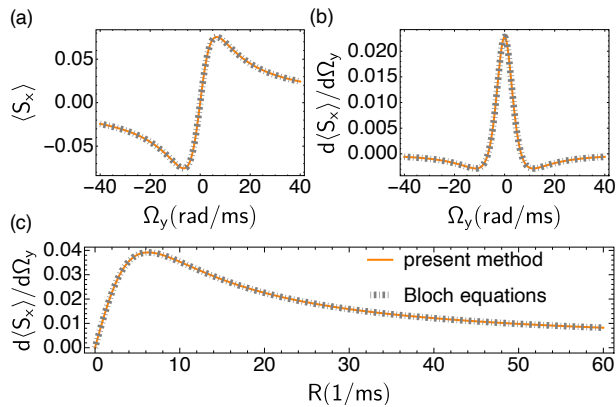


FIG. 3. (a) Magnetometer response  $\langle S_x \rangle$  as a function of  $\Omega_y$  for  $\Omega_z = 2\pi \times 1$  kHz. The optical pumping and randomization rates are  $R = 2000/\text{sec}$  and  $\Gamma = 100/\text{sec}$ , respectively. Dashed lines show analytic Bloch equation solutions. (b) Rate of change of  $\langle S_x \rangle$  with  $\Omega_y$ . The entire response in (a) and (b) has been calculated by the same two diagonalizations [Eq. (18)]. (c) The magnetometer sensitivity versus  $R$ , computed analytically by Eq. (19) using two diagonalizations.

[Eq (11b)]:

$$\rho_\delta = \sum_\lambda \frac{1}{1 + \lambda\delta} (\mathbf{r}_\lambda \mathbf{l}_\lambda^T) \rho_0 \quad (15)$$

where  $\rho_0$  is the solution at  $\delta = 0$  (or equivalently  $\Delta = -\omega_m$ ). Fig. 2 shows the steady state phonon number  $\langle n \rangle_m$  versus the detuning  $\Delta$ , computed using the present method (orange) and numerical diagonalization. In the numerical diagonalization approach, a new  $\mathcal{L}$  is initialized for every  $\Delta$ , and the steady state is found by numerically computing the nullspace for that  $\mathcal{L}$ . Using the present method, on the other hand, only two diagonalizations (that of  $\mathcal{L}_0$  and  $\mathcal{L}_0^- \mathcal{L}_1$ ) were used to generate the entire solution for the 121 different values of  $\Delta$  plotted [Eq. (15)]. Both methods are in excellent agreement with each other. Excluding the initial overhead taken to diagonalize  $\mathcal{L}_0$  and  $\mathcal{L}_0^- \mathcal{L}_1$ , the present solution [Eq. (15)] achieves one order of magnitude speedup in generating the steady state for a given  $\delta$ , compared to solving repeatedly for the nullspace.

## V. EXAMPLE 2: MAGNETOMETRY

We next consider a different problem, the magnetic response of  $^{87}\text{Rb}$  atoms in an optically pumped buffer gas. The Hamiltonian is [40]

$$H = \frac{\omega_0}{I + 1/2} \mathbf{S} \cdot \mathbf{I} + \gamma_S (S_y B_y + S_z B_z) = H_0 + \Omega_y S_y \quad (16)$$

where  $S = 1/2$  is the electron spin,  $I = 3/2$  is the nuclear spin, and  $\omega_0 = 2\pi \times 6.8$  GHz is the hyperfine splitting. Atoms are subjected to optical pumping along the  $z$ -axis at a rate  $R$  and electron spin-randomization collisions

at a rate  $\Gamma$ . The  $64 \times 64$  Liouville superoperator is  $\mathcal{L} = \mathcal{L}_0 + \Omega_y \mathcal{L}_1$  in the form of Eq. (2) with Lindblad operators

$$\{L_1, \dots, L_5\} = \left\{ \sqrt{\Gamma} S_x, \sqrt{\Gamma} S_y, \sqrt{\Gamma} S_z, \sqrt{R} S_+, \sqrt{R} S_z \right\} \quad (17)$$

This is a model of a low-field magnetometer, including the full hyperfine structure. As in the previous example, we can find the complete non-linear response of the atoms to the transverse magnetic field by first diagonalizing  $\mathcal{L}_0$  numerically, constructing its generalized inverse  $\mathcal{L}_0^-$ , and then numerically diagonalizing  $\mathcal{L}_0^- \mathcal{L}_1$  to find its eigenvalues  $\lambda$  and the corresponding right and left eigenvectors,  $\mathbf{r}_\lambda$  and  $\mathbf{l}_\lambda$ . From these we again construct the propagator

$$G_\Omega = \sum_\lambda \frac{1}{1 + \lambda\Omega_y} (\mathbf{r}_\lambda \mathbf{l}_\lambda^T) \quad (18)$$

to enable finding the steady-state density matrix for arbitrary  $\Omega_y$  from the nullspace  $\rho_0$  of  $\mathcal{L}_0$ . We re-emphasize that the calculation is non-perturbative, and with two matrix diagonalizations the steady-state density is completely determined for arbitrary values of  $\Omega_y$ . Fig. 3 (a) shows the magnetometer response  $\langle S_x \rangle$  as a function of the field  $\Omega_y$ , superposed on the steady-state solution to the Bloch equations (cf. Appendix F1 for the analytic solution). There is excellent agreement between the present approach and the analytic solution for all values of  $\Omega_y$ . As described previously, this method also allows for analytic operations (e.g., differentiation) to be done exactly without the need for numerical discretization or sampling. Fig. 3 (b) shows the rate of change of  $\langle S_x \rangle$  versus  $\Omega_y$ , computed by directly taking the derivative of the propagator [Eq. (18)] with respect to  $\Omega_y$ .

In certain cases, this approach allows for analytic optimization, even when only numerical steady-state solutions are available. As an example, consider the magnetometer response given by  $d\langle S_x \rangle/d\Omega_y = \text{vec}(S_x) \cdot \partial \rho(R, \Omega_y = 0)/\partial \Omega_y$ . This measures the magnetometer sensitivity to the field  $\Omega_y$  as a function of  $R$ . To optimize for  $R$  by brute force, one needs to find the steady state  $\rho(R, \Omega_y)$  for a sample of  $R$  and  $\Omega_y$  (around  $\Omega_y = 0$ ), and then approximate the derivative as a finite difference. Alternatively, using this approach, we show how to obtain an exact analytic expression for  $\partial_\Omega \rho(R, \Omega_y = 0)$  as a function of  $R$ . This way, the magnetometer can directly be optimized for  $R$ . In Appendix F2, we show that the magnetometer sensitivity is given by

$$\begin{aligned} \frac{\partial \rho(R, 0)}{\partial \Omega_y} &= -\frac{\mathbb{1}}{\mathbb{1} + R\mathcal{L}_0^- \mathcal{L}_R} \mathcal{L}_0^- \mathcal{L}_\Omega \rho(R, 0) \\ &= -\frac{\mathbb{1}}{\mathbb{1} + R\mathcal{L}_0^- \mathcal{L}_R} \mathcal{L}_0^- \mathcal{L}_\Omega \frac{\mathbb{1}}{\mathbb{1} + R\mathcal{L}_0^- \mathcal{L}_R} \rho(0, 0) \end{aligned} \quad (19)$$

where  $\mathcal{L}_\Omega$  is the superoperator constructed from  $S_y$ , and  $\mathcal{L}_R$  is constructed from the Lindblad operators  $S_+$  and  $S_z$ , using Eq. (2).  $\rho(0, 0)$  is the steady state at  $\Omega_y = R = 0$ . Once all the quantities in equation above

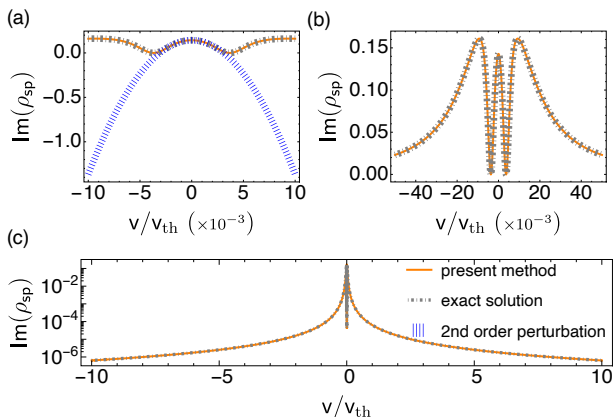


FIG. 4. (a)  $\text{Im}(\rho_{\text{sp}})$  as a function of velocity using the present method (orange solid), exact solution (dashed gray), and second order perturbation theory (dotted blue). The system parameters are: thermal velocity  $v_{\text{th}} = 169.5 \mu\text{m}/\mu\text{s}$ ,  $\Omega_1 = 2\pi \times 2 \text{ MHz}$ ,  $\Omega_2 = \Omega_3 = 2\pi \times 1 \text{ MHz}$  and  $\Gamma = 2\pi \times 6 \text{ MHz}$ . The modulation frequency is set to  $f = 0 \text{ MHz}$  here.  $k_1/2\pi = 1/(0.78 \mu\text{m})$  and  $k_2/2\pi = -1/(1.248 \mu\text{m})$ . The detunings are set in the EIT resonance regime  $\Delta = \delta = 0$ . (b) and (c) shows the agreement between present and the exact solution over larger domain range of  $v$ . Using the present method, the entire  $v$ -dependence has been generated by two diagonalizations.

are computed,  $\partial_{\Omega} \rho(R, \Omega_y = 0)$  is found for all  $R$ . This expression can be efficiently computed when expressed in the eigenbasis of  $\mathcal{L}_0^- \mathcal{L}_R$  (see Appendix B 3). Using Eq. (19), the maximum sensitivity is found at  $R = 6.28/\text{ms}$ . Fig. 3(c) shows excellent agreement between this approach [Eq. (19)] and the analytic solution for all  $R$ .

## VI. EXAMPLE 3: DOPPLER BROADENING OF A RYDBERG SENSOR

For a third example, we consider a multi-level system with time modulation, which experiences electromagnetically induced transparency (EIT) and Autler-Townes (AT) splitting. An ensemble of such atoms placed in a room-temperature vapor cell is used as a sensor to measure electromagnetic fields [15]. Since decoherence from Doppler broadening limits the performance of atomic sensors, simulating its effects accurately is an important problem [15, 41]. For sufficiently complicated systems, calculation of Doppler broadening presents a bottleneck in computation time and memory, increasing the simulation time by several orders of magnitude [14]. It is this problem that originally motivated this work. We begin by showing that the present method agrees with the exact solution in describing the non-trivial velocity dependence of the system. Then we calculate the Doppler broadening efficiently and accurately, without any sampling.

### A. Present method versus exact solution and perturbation theory

Consider a four-level ladder system in  $^{87}\text{Rb}$ , with a ground state S, an excited state P, and Rydberg states D and F. Let  $\Delta$  be the one-photon detuning between S and P,  $\delta$  the two-photon detuning between S and the Rydberg states. There is a probe field  $\Omega_1$  coupling S and P, and  $\Omega_2(t)$  is the control field coupling P and D. The field  $\Omega_3$  couples the Rydberg states D and F. The control field is time-modulated harmonically, i.e.,  $\Omega_2(t) = \Omega_2 \cos(\omega t)$ , where  $\Omega_2$  and  $\omega = 2\pi f$  are the modulation amplitude and frequency, respectively. P decays to S at a rate  $\Gamma = 2\pi \times 6 \text{ MHz}$ . The Hamiltonian and Lindblad operator for this system read [15]:

$$\begin{aligned}
 H &= -\Delta |p\rangle \langle p| - \delta |d\rangle \langle d| - \delta |f\rangle \langle f| + \frac{\Omega_1}{2} |s\rangle \langle p| \\
 &+ \frac{\Omega_2(t)}{2} |p\rangle \langle d| + \frac{\Omega_3}{2} |f\rangle \langle d| + \text{h.c.} \\
 L &= \sqrt{\Gamma} |s\rangle \langle p|
 \end{aligned} \tag{20}$$

from which  $\mathcal{L}_0$  can be readily constructed. At non-zero velocity  $v \neq 0$ , the atom experiences Doppler shift for the one- and two-photon detunings,  $\Delta \rightarrow \Delta - k_1 v$  and  $\delta \rightarrow \delta - k_2 v$ , where  $k_1$  and  $k_2$  are the effective wavenumbers for the one- and two-photon transitions. To determine the exact velocity dependence of the steady state, we proceed as before. First, we solve the zero-velocity problem by diagonalizing  $\mathcal{L}_0$  to obtain  $\rho_0$  and construct  $\mathcal{L}_0^-$ . Next, we diagonalize  $\mathcal{L}_0^- \mathcal{L}_1$  to get their eigenvalues and eigenvectors. Here,  $\mathcal{L}_1$  is the Doppler-shifted component of  $\mathcal{L}$  given by  $\mathcal{L}_1 = d\mathcal{L}_0(\Delta - k_1 v, \delta - k_2 v)/dv$ . Then  $\rho_v$  would be given by Eqs. (11a) and (11b) for all  $v$ . To be able to assess the exactness of the present method, we restrict this subsection to the case of no modulation (i.e.,  $f = 0$ ), for which an exact analytic solution can be found. The exact solution can be computed analytically by Mathematica's native Nullspace function for  $v = 0$ , and the  $v$ -dependence can be generated by applying the shifts  $\Delta \rightarrow \Delta - k_1 v$  and  $\delta \rightarrow \delta - k_2 v$  to the  $v = 0$  solution. In atomic sensors, the signal of interest is the imaginary component of the coherence between the ground and excited state,  $\text{Im}(\rho_{\text{sp}})$ , which is proportional to the absorption coefficient of the probe field. Fig. 4 shows  $\text{Im}(\rho_{\text{sp}})$  versus the velocity (normalized by the thermal velocity  $v_{\text{th}}$ ), using the present method, exact solution, and second-order perturbation theory (cf. Appendix C). The figure shows excellent agreement between the present approach and the exact solution, which is able to reproduce the exact EIT and AT structure at all scales of  $v$ . We reemphasize that only two diagonalizations were used to generate the entire  $v$ -dependence. The present approach works well beyond the domain of perturbation theory, where the latter only agrees with the exact solution in a very small interval of  $v/v_{\text{th}} \approx 5 \times 10^{-3}$ .

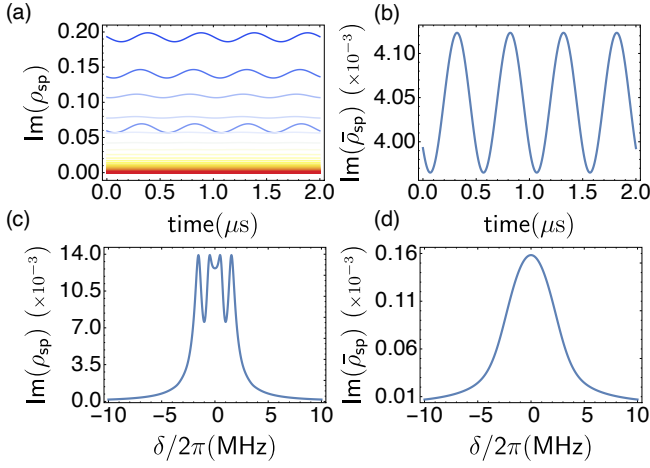


FIG. 5. (a)  $\text{Im}(\rho_{\text{sp}})$  as a function of time for different velocities from  $v = 0$  (dark blue) to  $v_{\text{th}} = 169.5 \mu\text{m}/\mu\text{s}$  (red). The system parameters are:  $\Omega_1 = 2\pi \times 2 \text{ MHz}$ ,  $\Omega_3 = 2\pi \times 1 \text{ MHz}$  and  $\Gamma = 2\pi \times 6 \text{ MHz}$ . The modulation amplitude and frequency are  $\Omega_2 = 2\pi \times 1 \text{ MHz}$  and  $f = 1 \text{ MHz}$ .  $k_1/2\pi = 1/(0.78 \mu\text{m})$  and  $k_2/2\pi = -1/(1.248 \mu\text{m})$ . The detunings are set in the EIT resonance regime  $\Delta = \delta = 0$ . (b) The Doppler averaged signal of (a), using the present method. Only two diagonalizations were used for the velocity averaging. (c) The peak-to-peak amplitude of  $\text{Im}(\rho_{\text{sp}})$  versus the two-photon detuning  $\delta$  at  $v = 0$ . (d) The Doppler averaged signal of (c), using the present approach.

### B. Time-periodic perturbation

The steady-state behavior of a system with harmonic perturbation,  $\Omega_2(t) = \Omega_2 \cos(\omega t)$  in our case, can be handled with Floquet analysis [1]. In the Floquet approach, the ansatz for  $\rho(t)$  is a Fourier decomposition in the harmonics of the modulating frequency  $\omega$ :  $\rho(t) = \sum_{m=-N}^N \rho_m \exp(im\omega t)$ . A solution is obtained once all  $\rho_m$  are found that satisfy the equations of motion. The sum above yields the exact solution when all the harmonics are included, i.e.,  $N = \infty$ . Practically, the number of higher-order harmonics are restricted to a finite integer  $N$ , which depends on the specific problem. The Liouville superoperator, constructed from  $H$  and  $L$ , can be decomposed into time-independent and -dependent parts as  $\mathcal{L} = \mathcal{L}' + \cos(\omega t)\mathcal{L}''$ . Using  $\cos(\omega t) = (e^{i\omega t} + e^{-i\omega t})/2$ , and plugging the Floquet ansatz into the master equation [Eq. (1)], we get the following equations relating the various harmonic components  $\rho_m$ :

$$(\mathcal{L}' + im\omega)\rho_m + \frac{\mathcal{L}''}{2}\rho_{m+1} + \frac{\mathcal{L}''}{2}\rho_{m-1} = 0 \quad (22)$$

If we construct a larger Floquet vector made from the harmonic components,  $\rho_F = (\rho_N, \rho_{N-1}, \dots, \rho_{-N})^T$ , then this can be rewritten as:

$$\mathcal{L}_F \rho_F = 0, \quad (23)$$

where the Floquet matrix  $\mathcal{L}_F$  is explicitly given by [Eq. (22)]

$$\mathcal{L}_F = \begin{bmatrix} \cdot & \cdot & \cdot & \cdot & \cdot & \cdot & \cdot & \cdot \\ \cdot & \mathcal{L}' + 2i\omega & \mathcal{L}''/2 & 0 & 0 & 0 & 0 & \cdot \\ \cdot & \mathcal{L}''/2 & \mathcal{L}' + i\omega & \mathcal{L}''/2 & 0 & 0 & 0 & \cdot \\ \cdot & 0 & \mathcal{L}''/2 & \mathcal{L}' & \mathcal{L}''/2 & 0 & 0 & \cdot \\ \cdot & 0 & 0 & \mathcal{L}''/2 & \mathcal{L}' - i\omega & \mathcal{L}''/2 & 0 & \cdot \\ \cdot & 0 & 0 & 0 & \mathcal{L}''/2 & \mathcal{L}' - 2i\omega & \mathcal{L}''/2 & \cdot \\ \cdot & \cdot & \cdot & \cdot & \cdot & \cdot & \cdot & \cdot \\ \cdot & \cdot & \cdot & \cdot & \cdot & \cdot & \cdot & \cdot \end{bmatrix} \quad (24)$$

Therefore, the Floquet ansatz has transformed the problem into a time-independent one, where the nullspace of  $\mathcal{L}_F$  gives  $\rho_F$ , which in turn gives  $\rho(t)$ . Here, we shall include up to the  $N = 4$  harmonic.

As before, for  $v \neq 0$ , the detunings are Doppler shifted as  $\Delta \rightarrow \Delta - k_1 v$  and  $\delta \rightarrow \delta - k_2 v$ . This changes the Hamiltonian and the corresponding Floquet matrix for every  $v$ . The observed signal is the coherence averaged over the Maxwell-Boltzmann distribution  $P(v)$  with a thermal velocity  $v_{\text{th}}$ . In Fig. 5(a), we plot  $\text{Im}(\rho_{\text{sp}})$  versus time at steady state for various velocities. The signal oscillates harmonically due to the time modulation of the control field. For larger detunings (i.e., large velocities) both the DC value of the signal and its amplitude get progressively smaller. Computing the Doppler broadening by brute force would involve sampling over  $v$  for hundreds of velocity classes and approximating the average by a Riemann sum.

To compute Doppler broadening by the present approach, we proceed as follows. We diagonalize  $\mathcal{L}_F$  at  $v = 0$  to find  $\rho_0$  and construct  $\mathcal{L}_F^-$ . Next, we construct  $\mathcal{L}_1$  by taking the Doppler shifted component of  $\mathcal{L}_F$ , i.e.,  $\mathcal{L}_1 = d\mathcal{L}_F(\Delta - k_1 v, \delta - k_2 v)/dv$ . Then we diagonalize  $\mathcal{L}_F^- \mathcal{L}_1$ . Finally, the exact Doppler averaged signal will be given by Eq. (12). Fig. 5(b) shows the Doppler averaged signal as a function of time, using the present method. Fig. 5(c) shows the peak-to-peak amplitude of the signal  $\text{Im}(\rho_{\text{sp}}(t))$  versus the two-photon detuning at zero velocity, and Fig. 5(d) shows the Doppler averaged signal. For each  $\delta$  in Fig. 5(d), only two diagonalizations are needed to do the velocity averaging exactly, without any sampling. As a comparison, we also do the averaging by uniformly sampling the Maxwell-Boltzmann distribution from  $-3v_{\text{th}}$  to  $3v_{\text{th}}$  with a spacing  $dv = 0.1$ , which captures 99.7% of the distribution. There is a good agreement between the present and the uniform sampling approach. We observe three orders of magnitude speedup in the computation time using the present method, compared to sampling.

## VII. DISCUSSION

We have presented a general non-perturbative approach to compute the exact state of certain open quan-

tum systems under time-independent or time-periodic perturbations. This work goes beyond previous perturbative frameworks [32, 33], where the present exact solution exists even when a corresponding perturbative solution does not. The main result is a derivation of the propagator  $G_v$  that generates the entire dependence of the steady state on the perturbation, just using two diagonalizations. The main technical result that enabled the construction of  $G_v$  is the use of a particular generalized inverse  $\mathcal{L}_0^-$  [Eq. (6)]. This generalized inverse naturally retains the normalization of the original unperturbed steady state via Eq. (7), where  $\mathbf{L}_0 = \text{vec}(\mathbf{1})$  and  $\mathbf{R}_0 = \boldsymbol{\rho}_0$  appear explicitly. This allows for efficient generation of the steady state, as well as exact analytic operations, without sampling or discretization. A particularly useful feature of this approach is that it works even if the steady state is only available numerically. We remark that it is in fact possible to construct a propagator  $G_v$  using a different generalized inverse, e.g., the Moore-Penrose inverse, which would also generate the exact state via  $\boldsymbol{\rho}_v = G_v \boldsymbol{\rho}_0$ . However, in this case, the steady state would need to be renormalized for every distinct  $v$ , and therefore  $\boldsymbol{\rho}_v$  would be a non-trivial function of  $v$ . This would make it challenging to do any analytic operations on  $\boldsymbol{\rho}_v$  efficiently or exactly. Therefore, we conclude that the present generalized inverse [Eq. (6)] is of central importance in the present theory.

The derivation of the propagator  $G_v$  relied on general assumptions, namely probability conservation during the time evolution, a unique steady state (see Ref. [42]

for sufficient conditions on uniqueness), and that  $\mathcal{L}$  and  $\mathcal{L}_0^- \mathcal{L}_1$  admit eigendecompositions. For some systems,  $\mathcal{L}$  does not admit an eigendecomposition [1, 43]. We leave it for future work to rigorously classify which class of open quantum systems satisfy the above assumptions, and hence can be handled with the present method. An interesting future direction is to extend the present approach to systems that do not admit such an eigendecomposition.

We have applied the present method on three non-trivial quantum systems, showing that it agrees with both exact and numerical solutions. In addition to being exact, we have demonstrated the method's utility for efficient numerical simulation, achieving a speedup of one to several orders of magnitude in certain cases. The present method is expected offer speedup for problems that require large sampling, when the computational time for diagonalizing the unperturbed system is much less than the time taken to repeatedly solve for the nullspace for different values of the perturbation. In particular, the present approach is well-positioned to offer speedup for problems involving ensemble averaging, e.g., inhomogeneous broadening calculations, because it completely avoids sampling.

#### ACKNOWLEDGMENTS

We would like to thank Anirudh Yadav for valuable discussions. This work was partially supported by the National Science Foundation (GOALI PHY-1912543 and 2016136 for the QLCI Hybrid Quantum Architectures and Networks).

- 
- [1] F. Campaioli, J. H. Cole, and H. Hapuarachchi, Quantum master equations: Tips and tricks for quantum optics, quantum computing, and beyond, *PRX Quantum* **5**, 020202 (2024).
  - [2] P. D. Nation, Steady-state solution methods for open quantum optical systems (2015), arXiv:1504.06768 [quant-ph].
  - [3] J. Cui, J. I. Cirac, and M. C. Bañuls, Variational matrix product operators for the steady state of dissipative quantum systems, *Phys. Rev. Lett.* **114**, 220601 (2015).
  - [4] F. Vicentini, A. Biella, N. Regnault, and C. Ciuti, Variational neural-network ansatz for steady states in open quantum systems, *Phys. Rev. Lett.* **122**, 250503 (2019).
  - [5] J. Dalibard, Y. Castin, and K. Mølmer, Wave-function approach to dissipative processes in quantum optics, *Phys. Rev. Lett.* **68**, 580 (1992).
  - [6] F. Vicentini, F. Minganti, A. Biella, G. Orso, and C. Ciuti, Optimal stochastic unraveling of disordered open quantum systems: Application to driven-dissipative photonic lattices, *Phys. Rev. A* **99**, 032115 (2019).
  - [7] F. Verstraete, J. J. García-Ripoll, and J. I. Cirac, Matrix product density operators: Simulation of finite-temperature and dissipative systems, *Phys. Rev. Lett.* **93**, 207204 (2004).
  - [8] P. D. Nation, J. R. Johansson, M. P. Blencowe, and A. J. Rimberg, Iterative solutions to the steady-state density matrix for optomechanical systems, *Phys. Rev. E* **91**, 013307 (2015).
  - [9] H. Weimer, A. Kshetrimayum, and R. Orús, Simulation methods for open quantum many-body systems, *Rev. Mod. Phys.* **93**, 015008 (2021).
  - [10] J. Johansson, P. Nation, and F. Nori, Qutip: An open-source python framework for the dynamics of open quantum systems, *Computer Physics Communications* **183**, 1760–1772 (2012).
  - [11] H. Chen and D. A. Lidar, Hamiltonian open quantum system toolkit, *Communications Physics* **5**, 10.1038/s42005-022-00887-2 (2022).
  - [12] H. Hogben, M. Krzystyniak, G. Charnock, P. Hore, and I. Kuprov, Spinach – a software library for simulation of spin dynamics in large spin systems, *Journal of Magnetic Resonance* **208**, 179 (2011).
  - [13] S. Krämer, D. Plankensteiner, L. Ostermann, and H. Ritsch, Quantumoptics.jl: A julia framework for simulating open quantum systems, *Computer Physics Communications* **227**, 109–116 (2018).
  - [14] B. N. Miller, D. H. Meyer, T. Virtanen, C. M. O'Brien, and K. C. Cox, Rydiqule: A graph-based paradigm for modeling rydberg and atomic sensors, *Computer Physics*



- Communications **294**, 108952 (2024).
- [15] R. Finkelstein, S. Bali, O. Firstenberg, and I. Novikova, A practical guide to electromagnetically induced transparency in atomic vapor, *New Journal of Physics* **25**, 035001 (2023).
- [16] P. Zanardi and L. Campos Venuti, Geometry, robustness, and emerging unitarity in dissipation-projected dynamics, *Phys. Rev. A* **91**, 052324 (2015).
- [17] F. Benatti, A. Nagy, and H. Narnhofer, Asymptotic entanglement and lindblad dynamics: a perturbative approach, *Journal of Physics A: Mathematical and Theoretical* **44**, 155303 (2011).
- [18] E. del Valle and M. J. Hartmann, Correlator expansion approach to stationary states of weakly coupled cavity arrays, *Journal of Physics B: Atomic, Molecular and Optical Physics* **46**, 224023 (2013).
- [19] C. Flindt, T. Novotný, A. Braggio, M. Sassetti, and A.-P. Jauho, Counting statistics of non-markovian quantum stochastic processes, *Physical Review Letters* **100**, 10.1103/physrevlett.100.150601 (2008).
- [20] M. Žnidarič, Relaxation times of dissipative many-body quantum systems, *Phys. Rev. E* **92**, 042143 (2015).
- [21] H. Li, H. Wu, W. Zheng, and W. Yi, Many-body non-hermitian skin effect under dynamic gauge coupling, *Phys. Rev. Res.* **5**, 033173 (2023).
- [22] V. Y. Shishkov, E. S. Andrianov, A. A. Pukhov, A. P. Vinogradov, and A. A. Lisyansky, Perturbation theory for lindblad superoperators for interacting open quantum systems, *Phys. Rev. A* **102**, 032207 (2020).
- [23] J. I. Cirac, R. Blatt, P. Zoller, and W. D. Phillips, Laser cooling of trapped ions in a standing wave, *Phys. Rev. A* **46**, 2668 (1992).
- [24] X. X. Yi, C. Li, and J. C. Su, Perturbative expansion for the master equation and its applications, *Phys. Rev. A* **62**, 013819 (2000).
- [25] A. A. Andrianov, M. V. Ioffe, E. A. Izotova, and O. O. Novikov, A perturbation algorithm for the pointers of franke–gorini–kossakowski–lindblad–sudarshan equation, *The European Physical Journal Plus* **135**, 531 (2020).
- [26] F. Reiter and A. S. Sørensen, Effective operator formalism for open quantum systems, *Phys. Rev. A* **85**, 032111 (2012).
- [27] E. M. Kessler, Generalized schrieffer-wolff formalism for dissipative systems, *Phys. Rev. A* **86**, 012126 (2012).
- [28] M. J. Kastoryano, F. Reiter, and A. S. Sørensen, Dissipative preparation of entanglement in optical cavities, *Phys. Rev. Lett.* **106**, 090502 (2011).
- [29] V. V. Albert, B. Bradlyn, M. Fraas, and L. Jiang, Geometry and response of lindbladians, *Phys. Rev. X* **6**, 041031 (2016).
- [30] V. V. Albert, Lindbladians with multiple steady states: theory and applications (2018), arXiv:1802.00010 [quant-ph].
- [31] A. Levy, E. Rabani, and D. T. Limmer, Response theory for nonequilibrium steady states of open quantum systems, *Phys. Rev. Res.* **3**, 023252 (2021).
- [32] A. C. Y. Li, F. Petruccione, and J. Koch, Perturbative approach to markovian open quantum systems, *Scientific Reports* **4**, 10.1038/srep04887 (2014).
- [33] A. C. Y. Li, F. Petruccione, and J. Koch, Resummation for nonequilibrium perturbation theory and application to open quantum lattices, *Phys. Rev. X* **6**, 021037 (2016).
- [34] Z. Lenarčič, F. Lange, and A. Rosch, Perturbative approach to weakly driven many-particle systems in the presence of approximate conservation laws, *Physical Review B* **97**, 10.1103/physrevb.97.024302 (2018).
- [35] W. Happer, Y.-Y. Jau, and T. G. Walker, Density matrix and liouville space, in *Optically Pumped Atoms* (John Wiley and Sons, Ltd, 2010) Chap. 4, pp. 33–47.
- [36] A. Ben-Israel and N. Y. Greville, *Generalized Inverses: Theory and Applications*, 2nd ed. (Springer, Berlin, Heidelberg, 2003) Chap. 1.
- [37] Qojulia, Optomechanical cavity, <https://docs.qojulia.org/examples/optomech-cooling/>.
- [38] M. Aspelmeyer, T. J. Kippenberg, and F. Marquardt, Cavity optomechanics, *Rev. Mod. Phys.* **86**, 1391 (2014).
- [39] J. Chan, T. P. M. Alegre, A. H. Safavi-Naeini, J. T. Hill, A. Krause, S. Gröblacher, M. Aspelmeyer, and O. Painter, Laser cooling of a nanomechanical oscillator into its quantum ground state, *Nature* **478**, 89–92 (2011).
- [40] T. G. Walker and W. Happer, Spin-exchange optical pumping of noble-gas nuclei, *Rev. Mod. Phys.* **69**, 629 (1997).
- [41] R. Behary, I. Novikova, E. Mikhailov, A. Gill, and A. Buikema, Rydberg raman-ramsey ( $r^3$ ) resonances in atomic vapor (2023), arXiv:2310.10615 [physics.atom-ph].
- [42] H. Spohn, Approach to equilibrium for completely positive dynamical semigroups of n-level systems, *Reports on Mathematical Physics* **10**, 189 (1976).
- [43] S. Kim and F. Hassler, Third quantization for bosons: symplectic diagonalization, non-hermitian hamiltonian, and symmetries, *Journal of Physics A: Mathematical and Theoretical* **56**, 385303 (2023).
- [44] L. S. Blackford, A. Petitet, R. Pozo, K. Remington, R. C. Whaley, J. Demmel, J. Dongarra, I. Duff, S. Hammarling, G. Henry, *et al.*, An updated set of basic linear algebra subprograms (blas), *ACM Transactions on Mathematical Software* **28**, 135 (2002).
- [45] F. Bloch, Nuclear induction, *Phys. Rev.* **70**, 460 (1946).
- [46] Y. Wang, Y. Niu, and C. Ye, Optically pumped magnetometer with dynamic common mode magnetic field compensation, *Sensors and Actuators A: Physical* **332**, 113195 (2021).

## Appendix A: Liouville superoperator formalism

We give a brief overview of the Liouville superoperator formalism used in this present work [35]. A vectorization  $\text{vec}(A)$  maps the operator  $A = \sum_{ij} A_{ij} |i\rangle \langle j|$  into the following column vector

$$\text{vec}(A) = \sum_{ij} A_{ij} |i\rangle \otimes |j\rangle \quad (\text{A1})$$

When applied to the density matrix,  $\rho = \sum_{ij} \rho_{ij} |i\rangle \langle j|$ , it gives the vectorized density matrix

$$\boldsymbol{\rho} = \text{vec}(\rho) = \sum_{ij} \rho_{ij} |i\rangle \otimes |j\rangle \quad (\text{A2})$$

It is useful to define a Frobenius inner product between two vectorized matrices:

$$\text{vec}(B)^\dagger \cdot \text{vec}(A) = \text{Tr}(B^\dagger A) \quad (\text{A3})$$

which can be proved from the vectorization definition [Eq. (A1)], and the orthonormality of the basis  $|i\rangle$  and  $|j\rangle$ . It follows from the above relation that the expectation value of a Hermitian operator  $A$  is given by

$$\text{Tr}(A\rho) = \text{vec}(A)^\dagger \cdot \rho \quad (\text{A4})$$

i.e., it is the dot product between the vectorization of  $A^*$  and  $\rho$ . An important special case is the trace of a density matrix

$$\text{Tr}(\rho) = \text{Tr}(\mathbb{1}\rho) = \text{vec}(\mathbb{1})^\text{T} \cdot \rho \quad (\text{A5})$$

where  $A^\text{T}$  denotes the transpose of  $A$ . Next, we recast the master equation into the superoperator form. Consider the Lindblad master equation [1]:

$$\dot{\rho}(t) = -i[H, \rho(t)] + \sum_k \left[ L_k \rho(t) L_k^\dagger - \frac{1}{2} \{L_k^\dagger L_k, \rho(t)\} \right] \quad (\text{A6})$$

Using the vectorization identity  $\text{vec}(ABC) = (A \otimes C^\text{T})\text{vec}(B)$ , this becomes

$$\frac{d\rho(t)}{dt} = \mathcal{L}\rho(t) \quad (\text{A7})$$

where the Liouville superoperator  $\mathcal{L}$  is given by

$$\begin{aligned} \mathcal{L} = & -i(H \otimes \mathbb{1} - \mathbb{1} \otimes H^\text{T}) \\ & + \sum_k (L_k \otimes L_k^* - \frac{1}{2} [L_k^\dagger L_k \otimes \mathbb{1} + \mathbb{1} \otimes L_k^\text{T} L_k^*]) \end{aligned} \quad (\text{A8})$$

For  $\mathcal{L}$  to be trace-persevering, it must obey the relation

$$\text{vec}(\mathbb{1})^\text{T} \cdot \mathcal{L} = 0 \quad (\text{A9})$$

To see this, take the dot product of  $\text{vec}(\mathbb{1})^\text{T}$  with the master equation [Eq. (A7)]:

$$\frac{d}{dt} \text{vec}(\mathbb{1})^\text{T} \cdot \rho(t) = \text{vec}(\mathbb{1})^\text{T} \cdot \mathcal{L}\rho(t) \quad (\text{A10})$$

Making the identification  $\text{Tr}(\rho(t)) = \text{vec}(\mathbb{1})^\text{T} \cdot \rho(t)$ , and imposing the normalization  $\text{Tr}(\rho(t)) = 1$  at all times and for any  $\rho$ , the left hand side must vanish for all  $t$ . This proves that the right hand side must vanish for any  $\mathcal{L}$ , i.e., this proves Eq. (A9). An important consequence is that the left null vector  $\mathbf{L}_0$  must be the same, i.e.,  $\mathbf{L}_0 = \text{vec}(\mathbb{1})^\text{T}$ , for all physical Lindbladians  $\mathcal{L}$ .

## Appendix B: Efficient construction of the generalized inverse and the propagator

### 1. Efficient construction of the generalized inverse

Let's denote the right and left eigenvectors matrices of  $\mathcal{L}_0$  as  $R = (\mathbf{R}_0, \dots, \mathbf{R}_N)$  and  $L = (\mathbf{L}_0, \dots, \mathbf{L}_N)$ , where the  $i$ th column contains the  $i$ th eigenvectors,  $\mathbf{R}_i$  and  $\mathbf{L}_i$ ,

respectively. Let  $G = (g_0, \dots, g_N)$  be the vector of eigenvalues  $g_i$ .  $L$  can be directly found by taking the inverse of the transpose of  $R$ , i.e.,  $L = (R^\text{T})^{-1}$ . We have observed that in some cases, if  $R$  is an ill-conditioned matrix, it might be numerically more accurate to compute the inverse operation in  $L = (R^\text{T})^{-1}$  using the Moore-Penrose inverse. The Moore-Penrose inverse is equivalent to the usual matrix inverse, if the matrix is invertible.

The generalized inverse in this work  $\mathcal{L}_0^-$  (not to be confused with the Moore-Penrose inverse) is given by

$$\mathcal{L}_0^- = \sum_{g \neq 0} \frac{1}{g} \mathbf{R}_g \mathbf{L}_g^\text{T} \quad (\text{B1})$$

$\mathcal{L}_0^-$  can be constructed as follows. Let  $R_-, L_-$ , and  $G_-$  be the matrices and vectors, excluding the nullspaces, i.e., they are  $R$  and  $L$  without  $\mathbf{R}_0$  and  $\mathbf{L}_0$ , and  $G_-$  is the vector without  $g = 0$ . Then we can succinctly rewrite  $\mathcal{L}_0^-$  [Eq. (6)] as

$$\mathcal{L}_0^- = (R_- * /G_-) L_-^\text{T} \quad (\text{B2})$$

where  $*/$  denotes the element-wise division of the matrix  $R_-$  and the vector  $G_-$ , i.e.,  $(\mathbf{R}_1/g_1, \dots, \mathbf{R}_N/g_N)$ .  $(R_- * /G_-) L_-^\text{T}$  denotes matrix multiplication between  $R_- * /G_-$  and  $L_-^\text{T}$ . Since matrix operations are implemented efficiently in basic linear algebra subprograms (BLAS) [44], which is implemented natively in many programming languages, Eq. (B2) is useful computationally as an efficient construction of the generalized inverse.

### 2. The generalized inverse for more than one variable

For the more general problem with several  $v_i$ , i.e.,

$$(\mathcal{L}_0 + v_1 \mathcal{L}_1 + \dots + v_n \mathcal{L}_n) \rho(v_1, v_2, \dots, v_n) = 0 \quad (\text{B3})$$

The corresponding propagator is given by

$$G(v_1, v_2, \dots, v_n) = \frac{1}{\mathbb{1} + \mathcal{L}_0^- \sum_{i=1}^n v_i \mathcal{L}_i} \quad (\text{B4})$$

This propagator acts on the zero-case solution  $\rho_0$  with  $\{v_i\} = 0$  to generate the general solution  $\rho(v_1, v_2, \dots, v_n)$ . In the present work, we restrict ourselves to the case of a single  $v$ .

### 3. Efficient construction of the propagator

$G_v$  is given by Eq. (4)

$$G_v = (\mathbb{1} + v \mathcal{L}_0^- \mathcal{L}_1)^{-1} \equiv \frac{1}{\mathbb{1} + v \mathcal{L}_0^- \mathcal{L}_1} \quad (\text{B5})$$

In the eigenbasis of  $\mathcal{L}_0^- \mathcal{L}_1$ , it is given by Eq. (11a)

$$G_v = \sum_\lambda \frac{1}{1 + \lambda v} r_\lambda l_\lambda^\text{T} \quad (\text{B6})$$

Let's denote the right and left eigenvectors matrices of  $\mathcal{L}_0^- \mathcal{L}_1$  as  $r = (\mathbf{r}_1, \dots, \mathbf{r}_N)$  and  $l = (\mathbf{l}_1, \dots, \mathbf{l}_N)$ , and the corresponding eigenvalues as the vector  $\Lambda = (\lambda_1, \dots, \lambda_N)$ . The left eigenvectors can be computed as  $l = (r^T)^{-1}$ . In some problems, if  $r$  is an ill-conditioned matrix, it might be numerically more accurate to compute the inverse operation in  $l = (r^T)^{-1}$  using the Moore-Penrose inverse instead of the normal matrix inverse. Using these definitions,  $G_v$  can be rewritten compactly as

$$G_v = [r * / (1 + v\Lambda)] l^T \quad (\text{B7})$$

where  $*/$  denotes the element-wise division of  $r$  and  $(1 + v\Lambda)$ , i.e.,  $(\mathbf{r}_1/[1 + v\lambda_1], \dots, \mathbf{r}_N/[1 + v\lambda_N])$ . Note that the scalar 1 is added to every element of the vector  $v\Lambda$  in the denominator. Next, we rewrite  $G_v$  further in a way that will prove computationally efficient. Using the identity  $1/(1 + \lambda v) = 1 - \lambda v/(1 + \lambda v)$  in Eq. (B6) and the completeness relation  $\sum_\lambda (\mathbf{r}_\lambda \mathbf{l}_\lambda^T) = \mathbb{1}$ , we can rewrite  $G_v$  as:

$$G_v = \mathbb{1} - \sum_\lambda \frac{\lambda v}{1 + \lambda v} \mathbf{r}_\lambda \mathbf{l}_\lambda^T \quad (\text{B8})$$

In this form, it is clear that the second term vanishes for all  $\lambda = 0$ , i.e., the nullspace of  $\mathcal{L}_0^- \mathcal{L}_1$  does not contribute to  $G_v$ . If we denote  $r_-$ ,  $l_-$ , and  $\Lambda_-$  as the matrices and vectors excluding all the zero eigenvectors/values from  $r$ ,  $l$ , and  $\Lambda$ , then we get:

$$G_v = \mathbb{1} - [v r_- * \Lambda_- / (1 + v\Lambda_-)] l_-^T \quad (\text{B9})$$

where  $r_- * \Lambda_- / (1 + v\Lambda_-)$  denotes the element wise multiplication of  $r_-$  and  $\Lambda_- / (1 + v\Lambda_-)$ . Typically  $\mathcal{L}_0^- \mathcal{L}_1$  has a large nullspace, and so Eq. (B9) is more computationally efficient than unnecessarily including the nullspaces [Eq. (B7)].

### Appendix C: The relation between the present approach and perturbation theory

Here, we elaborate on the connection between the present work and perturbation theory of open quantum systems [32]. We have shown that the exact solution for an arbitrary  $v$  is given by Eq. (10)

$$\rho_v = \frac{\mathbb{1}}{\mathbb{1} + v\mathcal{L}_0^- \mathcal{L}_1} \rho_0 \quad (\text{C1})$$

Expanding  $\rho_v$  in powers of  $v$  gives

$$\rho_v = \left[ \sum_{n=0}^{\infty} v^n (-\mathcal{L}_0^- \mathcal{L}_1)^n \right] \rho_0 \quad (\text{C2})$$

Truncating this series up to the Mth order gives the perturbative steady state up to the Mth order:

$$\rho_v^{(m)} = \left[ \sum_{n=0}^M v^n (-\mathcal{L}_0^- \mathcal{L}_1)^n \right] \rho_0 \quad (\text{C3})$$

Note that even though there is a finite-order truncation,  $\rho_v^{(m)}$  under the present method is still normalized because  $\mathcal{L}_0^-$  preserves the norm. To see this, compute the trace:

$$\begin{aligned} \text{Tr}(\rho_v) &= \text{vec}(\mathbb{1})^T \cdot \rho_v^{(m)} = \\ &= \text{vec}(\mathbb{1})^T (\mathbb{1} - v\mathcal{L}_0^- \mathcal{L}_1 + \dots + (-v\mathcal{L}_0^- \mathcal{L}_1)^m) \rho_0 \end{aligned} \quad (\text{C4})$$

The first term is  $\text{vec}(\mathbb{1})^T \cdot \rho_0 = 1$ , since  $\rho_0$  is normalized by construction. For higher-order terms,  $\text{vec}(\mathbb{1})^T \mathcal{L}_0^- = 0$ , since  $\text{vec}(\mathbb{1})^T = \mathbf{L}_0$  is the left nullspace vector for any quantum system, and  $\mathcal{L}_0^-$  [Eq. (6)] excludes the null space by construction. This shows that  $\rho_v^{(m)}$  is normalized for any order  $m$ .

Eq. (C3) is similar to density-matrix perturbation theory (dubbed Density matrix PT) in Ref. [32], with the difference that the other authors use the Moore-Penrose inverse for their generalized inverse. Density matrix PT suffers from the truncated density matrix  $\rho_v^{(m)}$  being potentially non-positive for certain parameters [32]. In Ref. [33], the authors extend their finite-order perturbation theory, where they do a partial resummation of their perturbative series by decomposing  $(-v\mathcal{L}_0^- \mathcal{L}_1)^n$  into diagonal and off-diagonal parts (in that work they use the same generalized inverse used in this present work  $\mathcal{L}_0^-$ ). They obtain a formal infinite series solution, given by Eq. (31) in their paper, where each term in the series contains corrections up to the infinite order. While Eq. (31) is formally an exact solution, for any practical calculations, this series has to be truncated to finite order, since the series is not in a closed analytic form.

The power series in Eq. (C2) converges if and only if the magnitude of all the eigenvalues of  $v\mathcal{L}_0^- \mathcal{L}_1$  is less than unity, i.e.,  $|v\mathcal{L}_0^- \mathcal{L}_1| < 1$ . In the case where  $|v\mathcal{L}_0^- \mathcal{L}_1| < 1$ , then a perturbative expansion [Eq. (C3)] exists, which converges to the non-perturbative result [Eq. (C1)] in the limit  $M \rightarrow \infty$ . If  $|v\mathcal{L}_0^- \mathcal{L}_1| > 1$ , on the other hand, then a perturbative expansion does not exist. However, even in that case, the non-perturbative result [Eq. (C1)] would still hold exactly for an arbitrary  $v$ , as was proved in Sec. III. Thus, this result is exact, non-perturbative, and it works even if a corresponding perturbation theory does not exist.

### Appendix D: Calculation of the Doppler broadening of a two-level system

Consider a two-level system, where an explicit analytic solution exists for the Doppler broadened absorption spectrum. Consider a ground and excited state,  $|g\rangle$  and  $|e\rangle$ , coupled by a field  $\Omega$  with a detuning  $\Delta$ . Let  $\Gamma$  be the decay rate of  $|e\rangle$ . Then the Hamiltonian and the Lindblad operators for this system are given by

$$H = -\Delta |e\rangle \langle e| + \frac{\Omega}{2} |e\rangle \langle g| + \frac{\Omega^*}{2} |g\rangle \langle e| \quad (\text{D1a})$$

$$L = \sqrt{\Gamma} |g\rangle \langle e| \quad (\text{D1b})$$

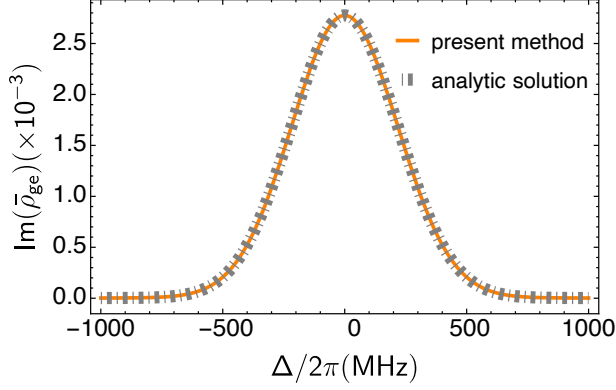


FIG. 6. The Doppler broadened absorption spectrum (up to a multiplicative constant) for a two-level system versus the detuning, using the analytic Voigt solution [Eq. (D4)] and the present method [Eq. (12)]. The system parameters are  $\Gamma = 2\pi \times 6$  MHz,  $v_{\text{th}} = 169.5 \mu\text{m}/\mu\text{s}$ ,  $k/2\pi = 1/(0.78\mu\text{m})$ , and  $\Omega = 2\pi \times 1$  MHz.

with a corresponding Liouville superoperator

$$\mathcal{L}_0 = \begin{bmatrix} -\Gamma & \frac{i\Omega}{2} & -\frac{i\Omega}{2} & 0 \\ \frac{i\Omega}{2} & -\frac{\Gamma}{2} + i\Delta & 0 & -\frac{i\Omega}{2} \\ -\frac{i\Omega}{2} & 0 & -\frac{\Gamma}{2} - i\Delta & \frac{i\Omega}{2} \\ \Gamma & -\frac{i\Omega}{2} & \frac{i\Omega}{2} & 0 \end{bmatrix} \quad (\text{D2})$$

where  $|g\rangle = (0, 1)^T$  and  $|e\rangle = (1, 0)^T$ . The atomic state at steady state  $\rho_0$  is the nullspace vector of  $\mathcal{L}_0$ . For this system, it is well-known that the absorption spectrum  $\chi$  versus  $\Delta$  is a Lorentzian, with its width being determined by decay rate of the excited state and the intensity of the light field (i.e., power broadening):

$$\chi \sim \text{Im}(\rho_{ge}) = \frac{\Omega\Gamma}{\Gamma^2 + 4\Delta^2 + 2\Omega^2} \quad (\text{D3})$$

For an atom moving at a velocity  $v$ , the detuning  $\Delta$  gets Doppler-shifted as  $\Delta - kv$ , where  $k$  is the wavenumber of the light. An ensemble of atoms moving with different velocities at non-zero temperature obey a Gaussian distribution, with thermal velocity  $v_{\text{th}}$ . The Doppler-broadened absorption spectrum  $\bar{\chi}$  is then calculated by averaging all the  $v$ -dependent solutions of  $\chi$  over that distribution. Applying this procedure on Eq. (D3) gives the Doppler-broadened spectrum:

$$\text{Im}(\bar{\rho}_{ge}) = \frac{\pi\Omega\Gamma}{2\sqrt{\Gamma^2 + 2\Omega^2}} V(\Delta; \sqrt{\Gamma^2 + 2\Omega^2}/2; kv_{\text{th}}) \quad (\text{D4})$$

where  $V(.;.;.)$  is the Voigt probability distribution, given by the convolution of a Lorentzian with a half width at half maximum (HWHM) =  $\sqrt{\Gamma^2 + 2\Omega^2}/2$  and a Gaussian with a standard deviation =  $kv_{\text{th}}$ .

Using the present approach, we directly obtain the averaged solution by applying Eq. (12). First, we solve the zero-velocity problem by diagonalizing  $\mathcal{L}_0$  to obtain  $\rho_0$  and construct  $\mathcal{L}_0^-$  [Eq. (B2)]. Next, we diagonalize  $\mathcal{L}_0^- \mathcal{L}_1$  to obtain their eigenvalues and eigenvectors. Here,  $\mathcal{L}_1$  is the Doppler shifted component of  $\mathcal{L}$  given by  $\mathcal{L}_1 = d\mathcal{L}_0(\Delta - kv)/dv$ :

$$\mathcal{L}_1 = \begin{bmatrix} 0 & 0 & 0 & 0 \\ 0 & -ik & 0 & 0 \\ 0 & 0 & ik & 0 \\ 0 & 0 & 0 & 0 \end{bmatrix} \quad (\text{D5})$$

Therefore, the problem of computing Doppler broadening exactly reduces to two diagonalization problems, as mentioned previously. Fig. 6 shows the Doppler broadened absorption spectrum calculated using the exact Voigt profile and the present method, using system parameters that are typical for  $^{87}\text{Rb}$  atoms. The present method and the analytic solution are in agreement, as expected.

### Appendix E: Ensemble average of the steady state over a Lorentzian

If  $v$  is distributed according to a Lorentzian then we have  $P(v) = \gamma/\pi(v^2 + \gamma^2)$ , where  $\gamma$  is the half-width at half-maximum (HWHM). This can be integrated analytically to give

$$\bar{\rho} = \sum_{\lambda} f(\lambda, \gamma) (\mathbf{r}_{\lambda} \mathbf{l}_{\lambda}^T) \rho_0 \quad (\text{E1})$$

where

$$f(\lambda, \gamma) = \begin{cases} \frac{i}{i + \gamma\lambda}, & \text{Im}(\lambda) > 0, \\ \frac{i}{i - \gamma\lambda}, & \text{Im}(\lambda) < 0. \end{cases} \quad (\text{E2})$$

### Appendix F: Magnetometer

#### 1. Bloch equations steady-state solution

The Bloch equation of a magnetometer describes the time evolution of the spin  $\mathbf{S}$  as a function of the field  $\mathbf{\Omega}$ , optical pumping  $\mathbf{R}$ , and spin relaxation  $\Gamma$ . It is given by [45, 46]

$$\frac{d}{dt} \mathbf{S} = \mathbf{\Omega} \times \mathbf{S} + \mathbf{R} \left( \frac{\hat{\mathbf{R}}}{2} - \mathbf{S} \right) - \Gamma \mathbf{S} \quad (\text{F1})$$

Solving for the steady state gives

$$\mathbf{S} = \frac{1}{2} \frac{\mathbf{R}\Gamma' + \mathbf{\Omega} \times \mathbf{R} + \mathbf{\Omega}(\mathbf{\Omega} \cdot \mathbf{R})/\Gamma'}{\mathbf{\Omega}^2 + \Gamma'^2} \quad (\text{F2})$$

where  $\Gamma' = \Gamma + |\mathbf{R}|$  and we take  $\hat{\mathbf{R}} = \hat{\mathbf{z}}$  and  $\mathbf{\Omega} = \Omega_y \hat{\mathbf{y}} + \Omega_z \hat{\mathbf{z}}$  in the present calculations.

## 2. Analytically optimizing the magnetometer response

We show how to get an analytic expression for  $\partial \boldsymbol{\rho}(R, \Omega_y = 0) / \partial \Omega_y$  as a function of  $R$ . At steady state, the system as a function of  $\Omega_y$  and  $R$  is given by

$$(\mathcal{L}_0 + R\mathcal{L}_R + \Omega_y\mathcal{L}_\Omega)\boldsymbol{\rho}(R, \Omega_y) = 0 \quad (\text{F3})$$

where  $\mathcal{L}_\Omega$  is constructed from  $S_y$  and  $\mathcal{L}_R$  is constructed from the Lindblad operators  $S_+$  and  $S_z$ . This has the solution (cf. Appendix B2):

$$\boldsymbol{\rho}(R, \Omega_y) = \frac{\mathbb{1}}{\mathbb{1} + R\mathcal{L}_0^- \mathcal{L}_R + \Omega_y\mathcal{L}_0^- \mathcal{L}_\Omega} \boldsymbol{\rho}(0, 0) \quad (\text{F4})$$

Letting  $B = \Omega_y\mathcal{L}_0^- \mathcal{L}_\Omega$  and  $A = R\mathcal{L}_0^- \mathcal{L}_R$ , we apply the matrix identity

$$\frac{1}{1 + A + B} = \frac{1}{1 + A} - \frac{1}{1 + A} B \frac{1}{1 + A + B} \quad (\text{F5})$$

on the previous expression. Since we are interested in small  $\Omega_y$ , we can employ the approximation

$$\frac{1}{1 + A + B} \approx \frac{1}{1 + A} - \frac{1}{1 + A} B \frac{1}{1 + A}, \quad \Omega_y \ll 1 \quad (\text{F6})$$

Applying this identity on  $\boldsymbol{\rho}(R, \Omega_y)$  gives:

$$\begin{aligned} \boldsymbol{\rho}(R, \Omega_y) \approx & \left( \frac{\mathbb{1}}{\mathbb{1} + R\mathcal{L}_0^- \mathcal{L}_R} \right. \\ & \left. - \frac{\mathbb{1}}{\mathbb{1} + R\mathcal{L}_0^- \mathcal{L}_R} \Omega_y \mathcal{L}_0^- \mathcal{L}_\Omega \frac{\mathbb{1}}{\mathbb{1} + R\mathcal{L}_0^- \mathcal{L}_R} \right) \boldsymbol{\rho}(0, 0) \end{aligned} \quad (\text{F7})$$

Taking the derivative with respect to  $\Omega_y$  gives the desired result:

$$\begin{aligned} \partial_\Omega \boldsymbol{\rho}(R, 0) &= -\frac{\mathbb{1}}{\mathbb{1} + R\mathcal{L}_0^- \mathcal{L}_R} \mathcal{L}_0^- \mathcal{L}_\Omega \boldsymbol{\rho}(R, 0) \\ &= -\frac{\mathbb{1}}{\mathbb{1} + R\mathcal{L}_0^- \mathcal{L}_R} \mathcal{L}_0^- \mathcal{L}_\Omega \frac{\mathbb{1}}{\mathbb{1} + R\mathcal{L}_0^- \mathcal{L}_R} \boldsymbol{\rho}(0, 0) \end{aligned} \quad (\text{F8})$$

This expression can be computed efficiently when expressed in the eigenbasis of  $\mathcal{L}_0^- \mathcal{L}_R$  (see Appendix B3). Moreover, it can be computed analytically as a function of  $R$  for systems sufficiently small in size (e.g., the magnetometer considered presently). Once  $\partial_\Omega \boldsymbol{\rho}(R, 0)$  is obtained analytically in  $R$ , it is straightforward to find  $R$  that maximizes the magnetometer response.